Grating-induced cyclotron-resonance anomaly in GaAs/$Al_xGa_{1-x}As$ heterostructures

Y. Zhao,* D. C. Tsui, M. B. Santos, and M. Shayegan
Department of Electrical Engineering, Princeton University, Princeton, New Jersey 08544

R. A. Ghanbari, D. A. Antoniadis, and H. I. Smith
Department of Electrical Engineering and Computer Science, Massachusetts Institute of Technology, Cambridge, Massachusetts 02139
(Received 7 October 1994)

We have investigated the far-infrared (FIR) cyclotron resonance (CR) of a two-dimensional electron gas (2DEG) in the presence of a grating coupler to excite plasmons in the 2DEG. We find that only when the coupling between the 2DEG and the metal grating is strong enough to excite 2D plasmons at $B=0$, the CR shows the anomalous broadening and splitting reported by Schlesinger *et al.* [Phys. Rev. B **30**, 435 (1984)]. Our experiment demonstrates that the anomaly must result from excitation of the 2DEG by spatially periodic components of the FIR field and confirms their original suggestion that it is of electro-electon interaction origin. However, to our knowledge there is still no theoretical explanation for the anomaly.

I. INTRODUCTION

Anomalous broadening and splitting of cyclotron resonance (CR) of the two-dimensional electron gas (2DEG) in GaAs/$Al_xGa_{1-x}As$ heterostructures were observed by Schlesinger *et al.*[1] in their early far-infrared (FIR) magneto-optical measurement. The experiment was done on samples supposed to be homogeneous by sweeping the FIR frequency with the external magnetic field (B) applied perpendicular to the sample surface. According to Kohn's theorem,[2] the FIR light can only excite CR of bare electrons in the homogeneous 2DEG and neither broadening nor splitting is expected. The observed anomaly is considered a breakdown of the Kohn theorem[3] and has been attributed to the electron-electron interaction in the 2DEG system. However, the nature of the physical mechanism that made it possible for the FIR light to access the electron-electron interaction effect in the 2DEG is unclear. In fact, how to relate the excitations of the interacting 2DEG system to the CR anomaly still remains an unsolved problem long after the appearance of several theoretical papers on this subject.[4–6]

Recently, Liu *et al.*[7] reported the observation of similar CR splitting in the 2DEG in a GaAs/$Al_xGa_{1-x}As$ heterostructure in the presence of a lateral surface superlattice potential, which was generated by applying a bias to a grid metal gate fabricated on the sample surface. This experiment was done by sweeping the B field at fixed FIR laser frequencies. Subsequently, Zhao *et al.*[8] continued the study on similarly prepared grid-gate samples and clarified, by using sweep-frequency measurements, that the splitting is accompanied by broadening. It is observed in samples without any bias on the gate, but not observed in samples from the same wafer without the grid gate. This result shows that the splitting is induced by the periodic modulation of the FIR radiation incident on the 2DEG by the grid metal gate.

We have since extended this study to samples with grating metal gates, which are commonly used as a radiation coupler to excite 2D plasmons by modulating the incident FIR radiation.[9–13] Since the amplitude of the spatially modulated component of the FIR radiation can be monitored directly by the absorption intensity of the 2D plasmons, the CR anomaly can be quantitatively related to it. We find that the grating coupler can indeed induce CR broadening and splitting and, as with the metal grids, the anomaly is not observed in samples from the same wafer without the grating coupler. The anomaly depends strongly on the ratio of the grating period a to the distance d from the metal grating to the 2DEG. The larger the a/d ratio, the stronger are the 2D plasma absorption and the CR anomaly. We conclude from this result that the CR anomaly is directly related to the intensity of the spatially modulated component of the FIR radiation at the 2DEG even though we have not been able to identify the physical mechanism or electronic process that gives rise to the anomaly. In this paper, we wish to present our data with the hope that they will provide additional constraints on and facilitate the search for a correct understanding of this physical phenomenon.

II. SAMPLE STRUCTURE AND EXPERIMENTAL DETAILS

Five samples with different metal-grating periods (a) made from three different wafers of GaAs/$Al_{0.35}Ga_{0.65}As$ heterostructures are measured: (1) $a=200$ nm from wafer M158 (M158G2), (2) $a=300$ nm from wafer M175 (M175G3), (3) $a=200$ nm from wafer M272 (M272G2), (4) $a=300$ nm from wafer M272 (M272G3), (5) $a=600$ nm from wafer M272 (M272G6). The wafers are grown by molecular-beam epitaxy (MBE) and their structures and growth sequences are illustrated in Fig. 1. The distance (d) from the wafer surface to the heterointerface is 78, 51, and 20 nm for wafers M158, M175, and M272, respectively. In Table I, we list a, d, the two-dimensional electron density (n_s), and mobility (μ) of each sample. The measured surface-to-2DEG distance for each sample

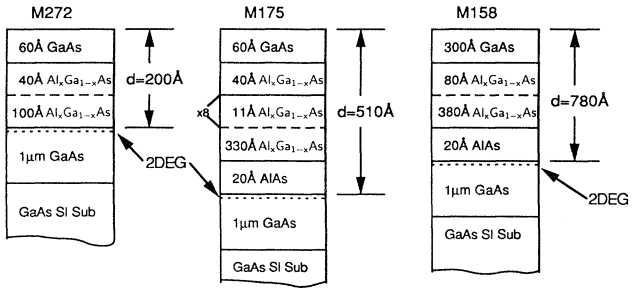

FIG. 1. Growth parameters of wafers M158, M175, and M272.

from the slope of the n_s versus gate voltage (V_G) curve, which is proportional to the capacitance of the wafer structure, agrees well with the growth parameter d for M158 and M175 within 15% experimental error. However, for M272, the distance measured is 30 nm (as indicted in parentheses) instead of 20 nm from the growth parameter. We always use the measured surface-to-2DEG distance in our calculations.

The grating pattern is fabricated by using x-ray lithography[14] and the metal grating is 10 nm Ti/20 nm Al. The width of the grating stripe is half of the grating period for all samples. Ohmic contacts are made at the four corners of each sample ($\sim 4\times 4$ mm^2 size). Three different gate structures are used on the three different samples to capacitively modulate the electron density. For M158G2 and M175G3, the grating coupler is the gate. In order to ensure an effective electron modulation (for getting a good enough absorption signal), a cross grating of 250 μm period is fabricated on each sample surface by photolithography for interconnecting the fine grating stripes. For M272G2 and M272G3, a continuous Ti film of 18 nm thick is evaporated all over the grating stripes to provide a semitransparent gate which allows us to modulate the electron density uniformly. For M272G6, a continuous back gate is made to provide the uniform density modulation. In this case, the sample is thinned to ~ 60 μm thick and is mounted on the surface of a wedged insulating GaAs substrate. A Ti film of ~ 5 nm thick is evaporated on the front surface of the wedged substrate as the back gate of the sample. The Ti film is specially treated to enhance its sheet resistance from ~ 300 Ω to ~ 3 KΩ in order to reduce its reflectivity and avoid interference between the Ti film and the sample front surface. Figure 2 is an illustration of the structure. All are wedged by 3° to avoid light interference.

TABLE I. Summary of sample parameters and experimental results.

	a/d ratio Low ⟶ High				
Samples	M158G2	M175G3	M272G2	M272G3	M272G6
n_s (cm^{-2})	2.4×10^{11}	2.2×10^{11}	3.9×10^{11}	4.7×10^{11}	4.7×10^{11}
μ (cm^2/V s)	1 000 000	500 000	60 000	60 000	60 000
a (nm)	200	300	200	300	600
d (nm)	78	51	20(30)	20(30)	20(30)
a/d ratio	2.6	6	6	10	20
I_P	0	0.015	0.02	0.032	0.09
A	1	2.2	1.3	1.5	3

All samples were cooled to 4.2 K and the absorption spectrum is taken by using a Fourier transform spectrometer with an 8 T superconducting magnet. The carrier density at $V_G=0$ is determined *in situ* from the quantum oscillations of the magnetoresistance of the 2DEG. In order to increase the detection sensitivity, we use double modulation[15] where the carrier density is modulated by modulating the gate voltage from zero to the conduction threshold V_T at the same time the FIR light is being chopped. Thus, for M158G2 and M175G3, the observed absorption spectrum is the difference between the absorption of the uniform 2DEG and the absorption of the 1D wire array. Since the features from the 2DEG and the 1D wires are well separated in the spectrum, the absorption of the 2DEG can be identified unambiguously.

III. DATA

In this section, we present our experimental data in the order of increasing a/d ratio of the samples starting with M158G2.

A. M158G2 [a/d = (200 nm)/(78 nm) ~ 2.6]

In Fig. 3, we plot its absorption spectra at $B=2.0$, 4.0, and 6.0 T. As a result of the double modulation,[15] the absorption features of the 200-nm-period 1D wire array (below the horizontal line) are mixed with the 2DEG spectra (above the horizontal line). The data are fitted using one oscillator for the CR absorption and one for the 1D wires. The fractional change in transmission is simply expressed as a function of the 2DEG conductivity σ_c and the conductivity σ_{1D} of the 1D wires:[16]

$$\frac{\Delta T}{T}=\frac{2/Y_0}{1+\sqrt{\varepsilon}}[\sigma_c(\omega)-\sigma_{1D}(\omega)] , \tag{1}$$

with

$$\sigma_c(\omega)=\frac{n_s e^2\tau_c}{m^*}\frac{1}{1+(\omega-\omega_c)^2\tau_c^2} , \tag{2}$$

and

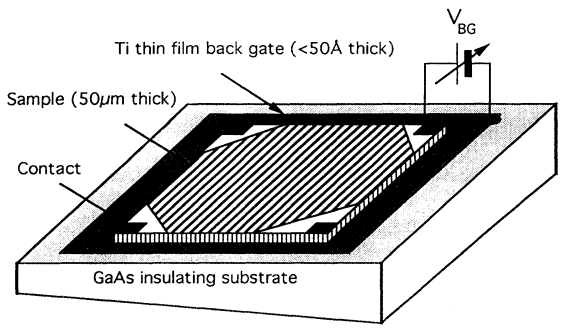

FIG. 2. The back gate structure for the density modulation.

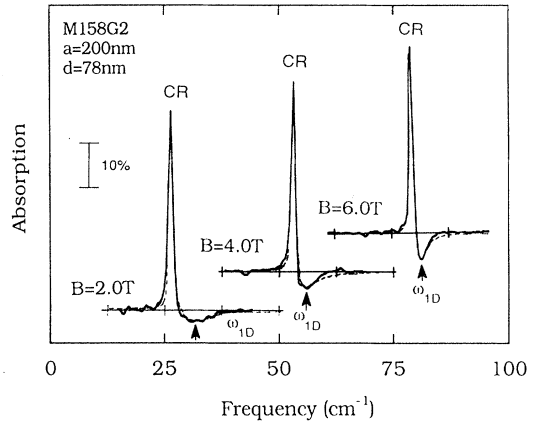

FIG. 3. Absorption spectra from M158G2 taken at $B=2.0$, 4.0, and 6.0 T. The feature above each horizontal line is from the uniform 2DEG (at $V_G=0$ V) and the feature below that is from the 1D wire array (at $V_G<V_T$). The dashed curves are the fits to a single oscillator for the CR and the 200-nm-period 1D wire absorptions.

$$\sigma_{1D}(\omega)=\frac{\bar{n}e^2\tau_{1D}}{m^*}\frac{\omega^2}{(\omega^2-\omega_{1D}^2)^2\tau_{1D}^2+\omega^2}\ . \tag{3}$$

Here, e is the electron charge, m^* is the electron effective mass, ω_c ($=eB/m^*$) is the CR frequency, ω_{1D} is the resonance frequency of the 1D wires, $\bar{n}$ is the effective areal electron density of 1D wires, τ_c and τ_{1D} are the electron scattering times of the 2DEG and 1D wires, and ε is the dielectric constant of GaAs. The resulting fits are shown by the dashed curves in Fig. 3. It is clear that only a sharp CR absorption is observed; neither the CR anomaly nor the 2D plasmon[9] with wave vector $q=2\pi/a$ is seen in this small-a/d-ratio sample. The τ_c obtained from fitting the spectra is 1×10^{-11} sec, different from τ_c ($=4\times10^{-11}$) obtained from the transport mobility. This difference results from the importance of small-angle scattering in the CR.[17]

B. M175G3 [a/d=(300 nm)/(51 nm)~6]

Figure 4 shows the absorption spectra taken at $B=0$, 1.5, 2.5, and 6.0 T. In this sample, the development of CR broadening is apparent. As the B field increases from low to high, the CR linewidth broadens, reaching a maximum at $B=2.5$ T, and then narrows for higher B. This broadening in linewidth is not seen in samples from the same wafer without the grating gate. Within the instrumental resolution of 2 cm^{-1}, no linewidth oscillation as a function of filling factor[4] is observed in samples without the grating gate. In Fig. 5, we plot the CR peak frequency with the grating gate (crosses) and without the grating gate (solid line) together with the linewidth of the grating sample (filled triangles) as a function of B.

In this sample, the grating a/d ratio is sufficiently large that the $q=2\pi/a$ 2D plasmon is observed at $B=0$. This is the weak peak at 47 cm^{-1}, indicted by the arrows in Fig. 4. The plasma frequency with wave vector q is given by[9]

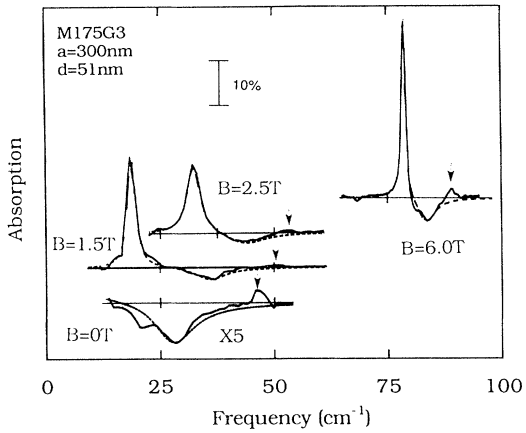

FIG. 4. Absorption spectra from M175G3 taken at $B=0$, 1.5, 2.5, and 6.0 T. The arrow indicates the $q=2\pi/a$ 2D plasma absorption induced by the grating coupler.

$$\omega_p=\left\{\frac{4\pi e^2 n_s}{m^*\varepsilon[1+\coth(qd)]}q\right\}^{1/2}\ . \tag{4}$$

Using $a=300$ nm, $d=51$ nm, $\varepsilon=12$, and $n_s=2.2\times10^{11}$ cm^{-2}, we obtain $\omega_p=46$ cm^{-1}, in good agreement with experiment. At $B\approx2$ T, level crossing of the magnetoplasmon with the second harmonic of the CR, $2\omega_c$, is observed. The filled circles in Fig. 5 are the B dispersion of the 2D magnetoplasmon. The dotted curves are the $2\omega_c$ and the $\omega_p(B)$ (given by $\omega_p(B)=[\omega_p^2(0)+\omega_c^2]^{1/2}$).

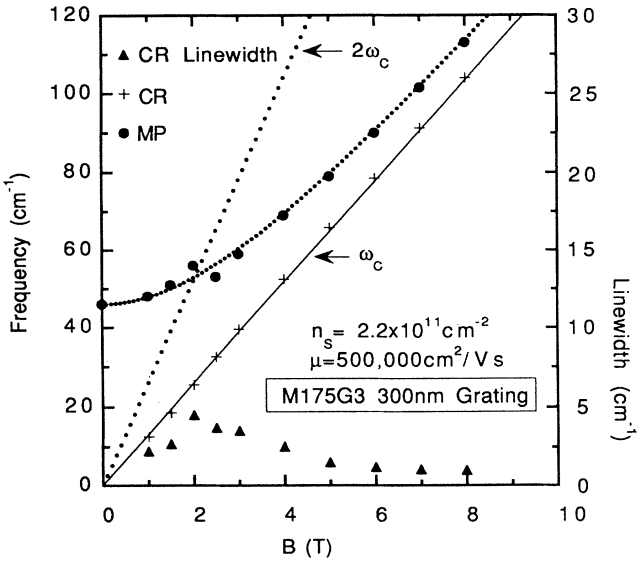

FIG. 5. The B dispersion of the CR (crosses) and the 2D plasma excitation ω_p (filled circles) for M175G3. The solid line indicates the CR positions measured from the sample from the same wafer without the grating coupler. The straight dotted line indicates $2\omega_c$ and the curved dotted line indicates $\omega_p(B)$. The CR linewidth as a function of B is also plotted (filled triangles).

C. M272G2 [a/d = (200 nm)/(33 nm) ~ 6]

The a/d ratio of this sample is the same as the sample in Sec. III B while the mobility is much lower ($\mu = 60\,000$ cm^2/V sec compared to 500 000 cm^2/V sec). Figure 6 shows several absorption spectra in the low-mobility sample. Here, anomalous broadening of the CR is barely noticeable, though the $q = 2\pi/a$ 2D plasmon is clearly seen at $B = 0$. The observed $\omega_p = 74$ cm^{-1} is in good agreement with the 75.5 cm^{-1} calculated from Eq. (4), using $a = 200$ nm, $d = 33$ nm, $\varepsilon = 12$, and $n_s = 3.9 \times 10^{11}$ cm^{-2}. In the presence of B, level crossing between $\omega_p(B)$ and $2\omega_c$ is resolved in the spectra, as indicated by the arrows in the figure. Data on this level crossing (filled circles), together with the CR linewidth (filled triangles) and the CR frequency (crosses) are shown in Fig. 7.

D. M272G3 [a/d = (300 nm)/(33 nm) ~ 10]

Figure 8 shows the absorption spectra of this large-a/d-ratio sample of equally low mobility. CR broadening is observed as a function of B. The linewidth increases as B increases, reaching a maximum at $B \sim 4$ T, and then narrows as B increases further. The CR (crosses) and its linewidth (filled triangles) are plotted in Fig. 9. The $q = 2\pi/a$ 2D plasmon is stronger in intensity than that from M275G3 and M272G2, as expected. Taking $a = 300$ nm, $d = 33$ nm, and $n_s = 4.7 \times 10^{11}$ cm^{-2}, Eq. (4) gives $\omega_p = 63$ cm^{-1}, while the experiment gives $\omega_p = 62$ cm^{-1}. The B dispersion of the plasmon, showing the level crossing of $2\omega_c$ and $\omega_p(B)$, is also plotted in Fig. 9.

E. M272G6 [a/d = (600 nm)/(33 nm) ~ 20]

This sample has the largest a/d ratio. The absorption spectra at $B = 0$, 2.0, 3.0, 3.75, 4.0, 5.0, and 8.0 T are plotted in Fig. 10. At $B = 0$, the 2D plasmon excitation, much stronger than that observed from the other grating samples, is observed at $\omega_p = 38$ cm^{-1}. This fact shows that the spatially periodic component of the FIR radiation at the 2DEG is indeed the strongest in this sample. At $B = 2.0$ T, one can see, in addition to the large CR peak, two small peaks on the high-frequency side of the CR, which are from the level crossing of $\omega_p(B)$ and $2\omega_c$. As B increases to 3.0 T, the CR broadens and only one magnetoplasmon peak is seen on its high-frequency side. AT $B = 3.75$ T, the CR becomes very broad and only a high-frequency shoulder is seen clearly. The linewidth of the CR reaches a maximum at $B = 4.0$ T and then decreases as B further increases (seen in the 5.0 and 8.0 T spectra). The CR broadening is more significant in this sample than in the other grating samples. The weak shoulder seen in the $B = 3.75$ T data indicates a splitting

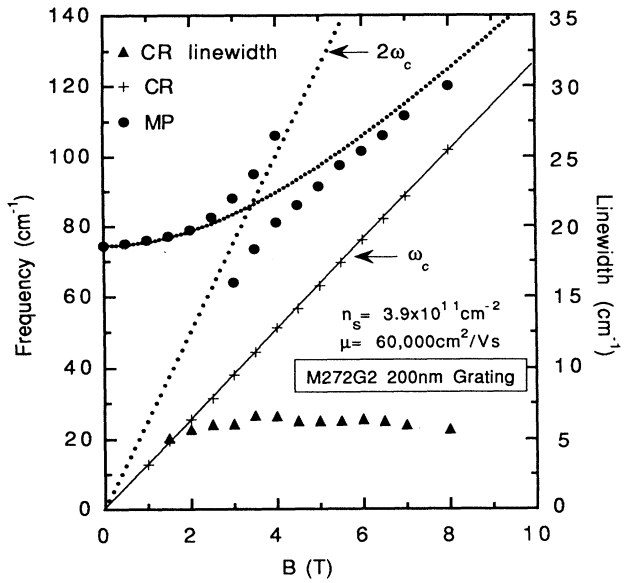

FIG. 7. The B dispersion of the CR (crosses) and the 2D plasma excitation (filled circles) for M272G2. The solid line indicates the CR positions measured from the sample from the same wafer without the grating coupler. The straight dotted line indicates $2\omega_c$ and the curved dotted line indicates $\omega_p(B)$. The CR linewidth as a function of B is also plotted (filled triangles).

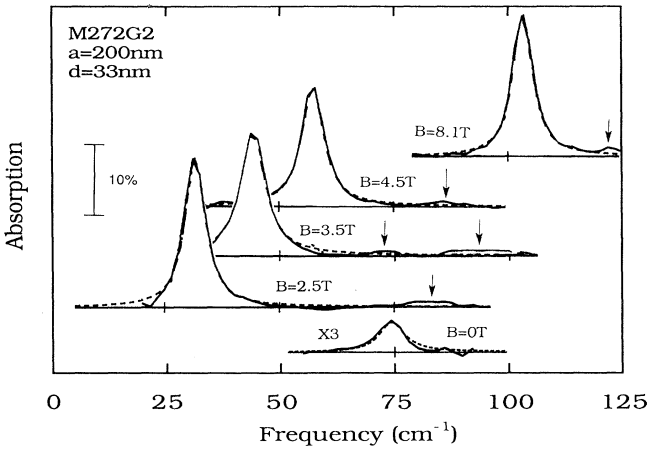

FIG. 6. Absorption spectra from M272G2 taken at $B = 0$, 2.5, 3.5, 4.5, and 8.1 T. The dashed curves are the fit to a single oscillator for the CR only.

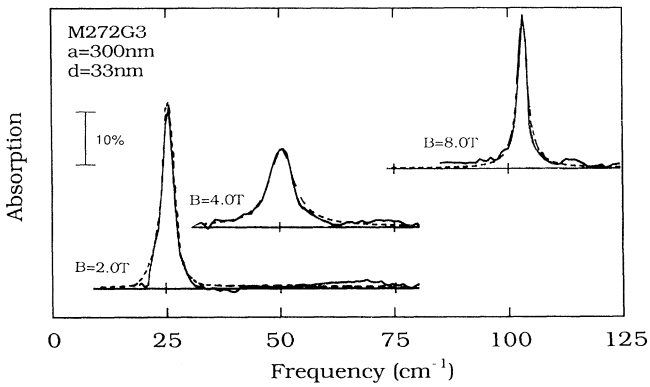

FIG. 8. Absorption spectra from M272G3 taken at $B = 2.0$, 4.0, and 8.0 T.

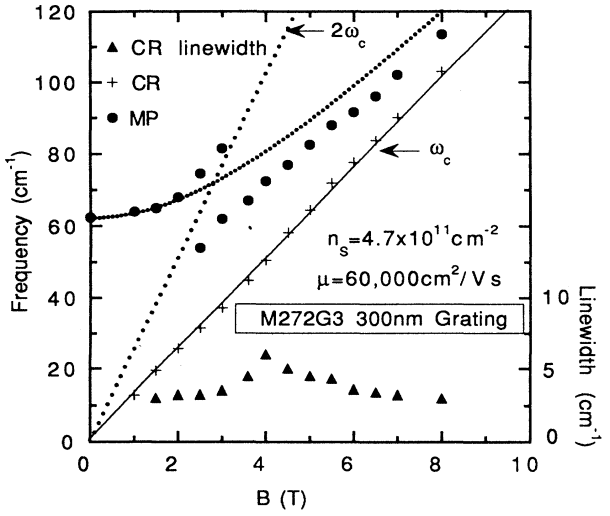

FIG. 9. The B dispersion of the CR (crosses) and the 2D plasma excitation (filled circles) for M272G3. The solid line indicates the CR positions measured from the sample from the same wafer without the grating coupler. The straight dotted line indicates $2\omega_c$ and the curved dotted line indicates $\omega_p(B)$. The CR linewidth as a function of B is also plotted (filled triangles).

of the CR (marked by an arrow). The spectrum nearby is asymmetric, and cannot be fitted by using the single-oscillator model. In fact, if the two sides of the CR at $B=3.75$ or 4.0 T are fitted together with two separate oscillators (as shown by the dashed curves), the difference (dotted curve) between the experimental spectrum (solid curve) and the fitted curve indicates that a third oscillator is needed for a complete fit. In Fig. 11, we plot the B dispersion of the CR (crosses) and its linewidth (filled triangles). The splitting is seen around $B=4.0$ T where the CR reaches a maximum in linewidth.

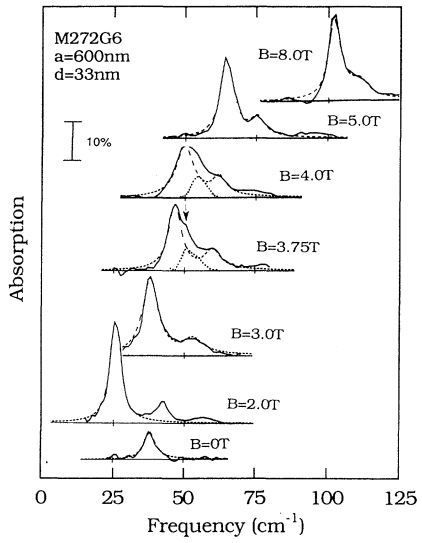

FIG. 10. Absorption spectra from M272G6 taken at $B=0$, 2.0, 3.0, 3.75, 4.0, 5.0, and 8.0 T.

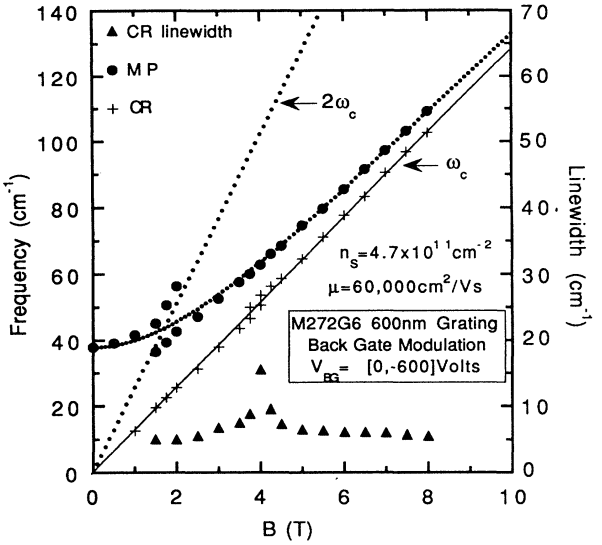

FIG. 11. The B dispersion of the CR (crosses) and the 2D plasma excitation (filled circles) for M272G6. The solid line indicates the CR positions measured from the sample from the same wafer without the grating coupler. The straight dotted line indicates $2\omega_c$ and the curved dotted line indicates $\omega_p(B)$. The CR linewidth as a function of B is also plotted (filled triangles).

IV. DISCUSSION

In this section, we discuss in some detail the relevance of our experiment to the anomaly reported by Schlesinger *et al.*[1] First, we note that the integrated absorption intensity in all our samples is found to be constant, independent of B and of the anomalous broadening and splitting. In Fig. 12, we plot the integrated intensity of each spectrum taken from sample M272G6 against the B

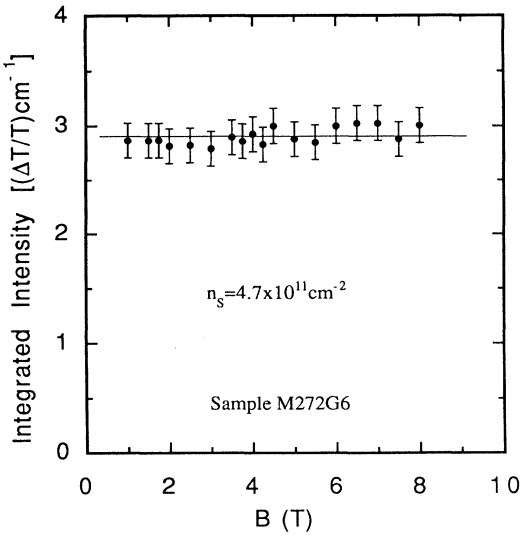

FIG. 12. The integrated intensity of each absorption spectrum (total area of the spectrum) taken from the sample M272G6 is plotted against B.

field. It is clear that, within our experimental error, the intensity is constant over the range of B we studied and thus satisfies the sum rule. One may, therefore, conclude that the observed anomaly must have its origin in the 2DEG. Secondly, the anomaly is not observed in our samples from the same wafer without the metal grating, and also not in the sample with a grating of small a/d ratio, in which the amplitude of the periodic component of the FIR field is negligible at the interface. No CR linewidth oscillation as a function of filling factor is observed in all our ungated samples within our instrumental resolution of 2 cm^{-1}.[3] This observation is consistent with the result from our previous experiment on grid-gate samples and also with the more recent CR experiments on very-high-mobility samples,[18] showing no such anomalies. Including results from our samples not reported in this paper, the filling factor for the linewidth maximum can be anywhere from $\nu=3$ to 5, not necessarily an integer. Thus the observed anomaly has a different origin from that reported by Englert *et al.* and Chou, Tsui, and Weimann.[3] These observations, when taken together, further confirm the correctness of the original suggestion of Schlesinger *et al.* that the anomaly is of electron-electron interaction origin and its observation results from a breakdown of the Kohn theorem. In our samples, the breakdown of Kohn's theorem is caused by the periodic metal grating fabricated on top of the sample. In their case, we believe, it is due to the oval defects, which are common in $GaAs/Al_{0.35}Ga_{0.65}As$ heterostructures grown in those days.

The amplitude of the periodic component of the FIR field at the 2DEG is related directly in our samples to the intensity of the 2D plasma resonance observed at $B=0$. We use I_p, the integrated absorption intensity of the plasma resonance normalized by the 2DEG density, as a measure of this field. The bottom two lines in Table I summarize our results on I_p and A, the strength of the anomaly, given by

$$A=\Delta\nu_m/\Delta\nu\ , \tag{5}$$

where $\Delta\nu_m$ is the maximum linewidth. It is clear that the observed anomaly correlates well with the strength of the plasma resonance. This correlation is specially apparent in the three samples having the same 2DEG mobility. The large value of A for M175G3 is due to its having a higher mobility and, therefore, narrower initial linewidth. On the other hand, we do not observe any linewidth dependence of the magnetoplasma on the CR linewidth broadening.

It is apparent from the above discussion that the anomaly must result from coupling of the 2DEG with the periodic component of the FIR radiation field at the interface. One distinct possibility is that the broadening is the result of unresolved splitting due to the crossing of the CR branch with a not-yet-identified plasma branch, made accessible to the FIR by the periodic metal grating. This interpretation is consistent with observation of splitting in our sample with the largest a/d ratio and also with the fact that, at B below that for the broadening maximum, the CR peak is lower than that observed in samples from the same wafer without the grating, and higher at high B. The fact that the anomaly is much weaker in the lower-mobility sample of the same a/d ratio is also consistent with this conjecture. However, the lack of any observable dependence of the crossing B field, B_M, on the grating periodicity can only be reconciled with a magnetoplasma mode which is almost dispersionless in this small-q regime.

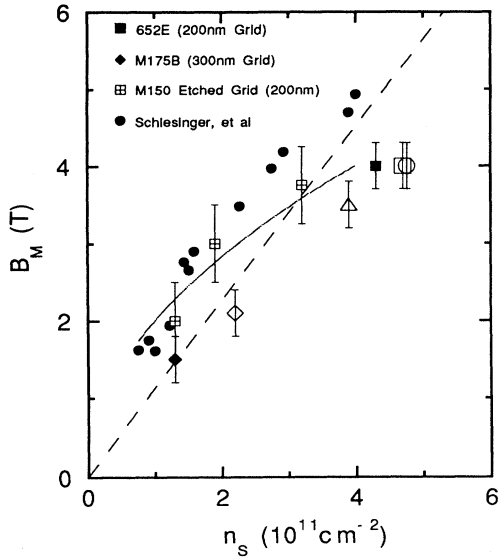

FIG. 13. B_M vs n_s data points for M175G3 (open diamond), M272G2 (open triangle), M272G3 (open square), and M272G6 (open circle). Data from our grid sample M175BG, grid sample 652E, by Zhao *et al.* (Ref. 8), etched grid M150, and the data by Schlesinger *et al.* (Ref. 1) are also plotted together for comparison. The dashed and solid lines indicate n and $\sqrt{n}$ dependence, respectively.

Finally, the functional form of the dependence of B_M on n_s is not yet clear. In Fig. 13, we plot the data from our grating as well as grid samples together with those of Schlesinger *et al.* While Schlesinger *et al.* fitted their data to a $\sqrt{n}$ dependence, it is clear from the plot that at this point we cannot yet be certain whether $\sqrt{n}$ or n should be preferred.

V. CONCLUSIONS

We have investigated the CR of the 2DEG in $GaAs/Al_{0.35}Ga_{0.65}As$ in the presence of a grating metal gate, with a grating period of 200, 300, or 600 nm, which is used as a radiation coupler to excite the 2D plasmons by modulating the incident FIR radiation. We find that only when the grating coupling is sufficiently strong to excite 2D plasmons at $B=0$ does the CR show the anomalous broadening and splitting reported by Schlesinger *et al.* The strength of the anomaly correlates well with the strength of the plasma resonance. Our experiment demonstrates that the anomaly must result from coupling of the 2DEG with spatially periodic components of the radiation field at the $GaAs/Al_{0.35}Ga_{0.65}As$ interface and further confirms the correctness of the suggestion of Schlesinger *et al.* that the anomaly is of electron-electron

interaction origin. A possible explanation, we believe, is crossing of the CR with a magnetoplasma branch. However, there is no solid theoretical backing for the explanation and, experimentally, we have not yet been able to identify the magnetoplasma branch and establish the anticrossing nature of the level structure, with the quality of the 2DEG in samples available to us at the present.

ACKNOWLEDGMENTS

This work is supported by the Air Force Office of Scientific Research under Grant No. AFOSR-910353 at Princeton University. The MIT portion of this work is sponsored by the Joint Services Electronics Program under Grant No. DAAL03-92-c-0001.

*Present address: Analog Devices, Inc., 831 Woburn Street, Wilmington, MA 01887.

[1]Z. Schlesinger, S. J. Allen, J. C. M. Hwang, P. M. Platzman, and N. Tzoar, Phys. Rev. B **30**, 435 (1984).

[2]W. Kohn, Phys. Rev. **123**, 1242 (1961).

[3]CR linewidth oscillation due to variation of screening as a function of Landau level filling factor ν ($=n_s h/eB$) and CR broadening in the $\nu<1$ extreme quantum limit have been reported by Th. Englert, J. C. Maan, Ch. Uihlein, D. C. Tsui, and A. C. Gossard, Solid State Commun. **46**, 545 (1983), and by M. J. Chou, D. C. Tsui, and G. Weimann, Phys. Rev. B **37**, 848 (1988), respectively. They are different from the anomalous broadening and splitting observed by Schlesinger *et al.*, in that they depend only on ν and are observable in the small-ν limit.

[4]A. H. MacDonald, J. Phys. C **18**, 1003 (1985).

[5]C. Kallin and B. I. Halperin, Phys. Rev. B **30**, 5655 (1984); **31**, 3635 (1985).

[6]A. H. MacDonald and C. Kallin, Phys. Rev. B **40**, 5795 (1989).

[7]C. T. Liu, K. Nakamura, D. C. Tsui, K. Ismail, D. A. Antoniadis, and Henry I. Smith, Surf. Sci. **228**, 527 (1990).

[8]Y. Zhao, D. C. Tsui, K. Hirakawa, M. Santos, M. Shayegan, R. A. Ghanbari, D. A. Antoniadis, and Henry I. Smith (unpublished).

[9]S. J. Allen, Jr., D. C. Tsui, and R. A. Logan, Phys. Rev. Lett. **38**, 980 (1977).

[10]E. Batke, D. Heitmann, J. P. Kotthaus, and K. Ploog, Phys. Rev. Lett. **54**, 2367 (1985), and references therein.

[11]T. N. Theis, Surf. Sci. **98**, 515 (1980).

[12]L. Zheng, W. L. Schaich, and A. H. MacDonald, Phys. Rev. B **41**, 8493 (1990).

[13]D. Liu and S. Das Sarma, Phys. Rev. B **44**, 9122 (1991).

[14]K. Ismail, D. A. Antoniadis, Henry I. Smith, C. T. Liu, K. Nakamura, and D. C. Tsui, J. Vac. Sci. Technol. B **7**, 2000 (1989).

[15]Y. Zhao, D. C. Tsui, M. Santos, M. Shayegan, R. A. Ghanbari, D. A. Antoniadis, Henry I. Smith, and K. Kempa, Phys. Rev. B **48**, 5249 (1993).

[16]To simplify the fitting (line shape only), we use the formula of σ_{1D} at $B=0$ T by choosing $\omega_{1D}(B)=[\omega_{1D}^2(B=0)+\omega_c^2]^{1/2}$. The proper form of σ_{1D} for $B\neq 0$ T is more complicated.

[17]S. Das Sarma and F. Stern, Phys. Rev. B **32**, 8442 (1985).

[18]M. Besson, E. Gornik, C. M. Engelhardt, and G. Weimann, Semicond. Sci. Technol. **7**, 1274 (1992).